Segregation and Phase Dynamics in Supported Bimetallic Nanoparticles

Michael S. Nashner   Final Seminar   September 2, 1997

The chemically activated nucleation and growth of nanoscale compound and alloy materials is of fundamental importance for applications involving such areas as heterogeneous catalysis, microelectronics, and advanced materials synthesis.[1-5] The rational design of nanoscale structures for improved technologies increasingly relies on developing a predictive understanding of these dynamical processes and of how they contribute to the phase behaviors of nanoscale systems. The limited understanding of these processes obtained to date reflects, in large part, the inherent difficulty of preparing and characterizing well-defined nanometer sized alloy and intermetallic phases for fundamental structural studies.[6-8]

Nanometer sized Pt-Ru particles supported on carbon have recently generated excitement because of their improved catalytic activity for the electroxidation of methanol in direct methanol fuel cells.[9-11] A detailed understanding of the compositional and size dependencies of the electrocatalytic reaction rates over the Pt-Ru nanoparticles remains to be realized, however. One of the challenges of such studies is the difficulty in preparing nanometer sized alloy particles with narrow distributions of size and composition .[11]

The use of molecular clusters as precursors for well defined nanoparticles has proven advantageous because they precombine the proper stoichiometry of metal atoms as a molecular complex.[12-14] The neutral complex $PtRu_5C(CO)_{16}$ was dispersed (1-2 wt% metal) on carbon black (ca. 200 m^2/g) and heated at 673 K in H_2 (1 h) to form bimetallic nanoparticles, hereafter referred to as [PtRu5]/C.[15] Figure 1(a) displays a representative dark field image of the [PtRu5]/C nanoparticles measured with a Vacuum Generators HB501 scanning transmission electron microscope (STEM). The metal particles have an average diameter of 1.6 nm and, most significantly, exhibit a very narrow size distribution.
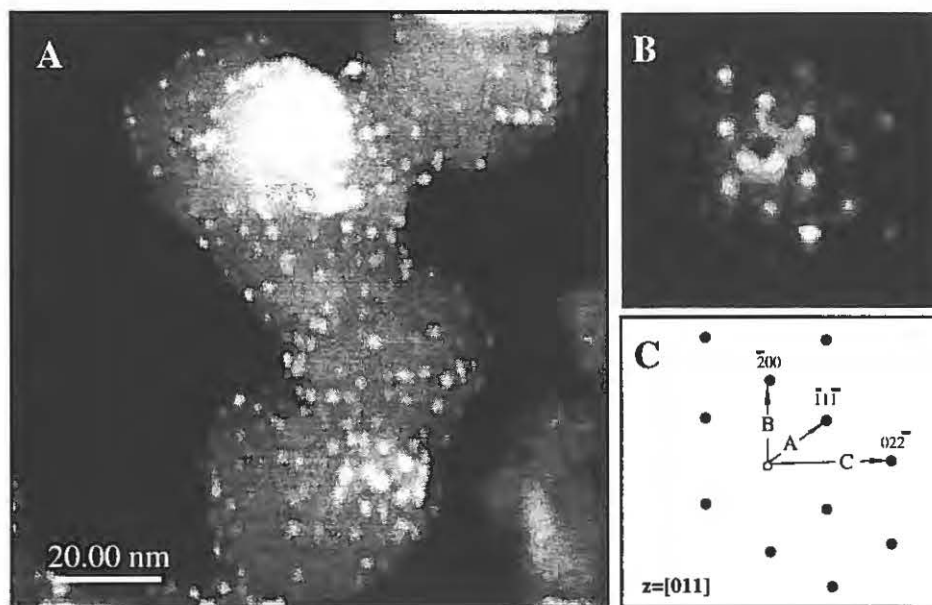

Figure 1. Dark field STEM image (a) of carbon-supported [PtRu5] nanoparticles. A representative microdiffraction image (b) measured from a single 1.5 nm [PtRu5] nanoparticle and indexed (c) to an fcc structure.

The composition and structure of individual nanoparticles were determined by atom probe energy dispersive X-ray analysis (EDX) and microdiffraction, respectively. These experiments were enabled by the high intensity and narrow electron beam (ca. 1 nm diameter) of the STEM. Compositional analysis of 240 nanoparticles indicated a Pt:Ru composition centered on the nominal 1:5 atomic%. Figure 1(b) displays a representative electron microdiffraction image measured from a single [PtRu$_5$]/C nanoparticle. This image and several others were indexed (Figure 1(c)) to a face-centered cubic (fcc) closest packed structure. It is extremely interesting to note that the bulk Pt-Ru phase diagram predicts that a 1 to 5 atomic% alloy would form a substitutional solid solution with an hexagonal close-packed (hcp) crystal structure.[16]

The local atomic microstructure of the [PtRu$_5$] nanoparticles was probed *in-situ* using X-ray absorption fine structure (EXAFS) spectroscopy.[17] The EXAFS data were collected at the National Synchrotron Light Source, located at the Brookhaven National Laboratory, using the UIUC/AT&T beamline X16C and a custom designed catalyst cell. The Pt L$_3$ (11564 eV) and Ru K (22117 eV) edge EXAFS data were collected from the [PtRu$_5$]/C nanoparticles at 190 K after reduction in H$_2$. The Fourier-transformed (*r*-space) data is shown in Figure 2. Consistent with the microdiffraction data, the shell structure (*r*-range 1.8 to 5.5 Å) exhibits a close-packed arrangement of metal atoms around Pt and Ru.
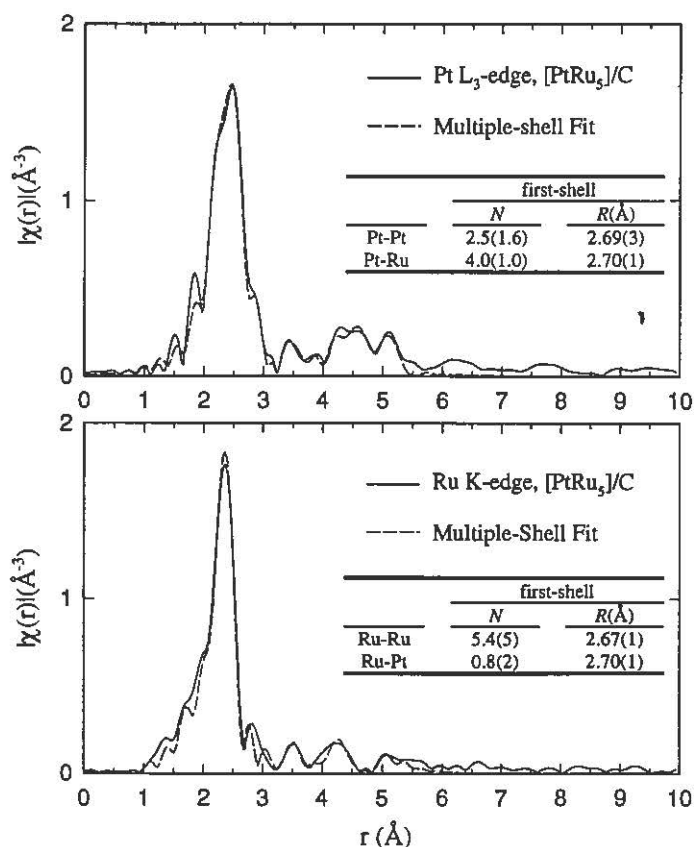

	first-shell	
	N	$R(\text{Å})$
Pt-Pt	2.5(1.6)	2.69(3)
Pt-Ru	4.0(1.0)	2.70(1)

	first-shell	
	N	$R(\text{Å})$
Ru-Ru	5.4(5)	2.67(1)
Ru-Pt	0.8(2)	2.70(1)

Figure 2. Pt and Ru EXAFS data measured from the [PtRu$_5$]/C nanoparticles at 190 K under H$_2$ (solid) and the multiple-shell fit results. The tables display the relevant first-shell structural parameters determined by the fitting analysis.

Quantitative structural parameters were determined by fitting the EXAFS data using a combination of reference and theoretical EXAFS signals.[18] The Pt and Ru EXAFS data were fit simultaneously from the first to the fourth shells (Figure 2) with an fcc structural model where the number of heterometallic bonding interactions was fixed in accordance with the 1:5 composition.

The local metal coordination environment, revealed by multiple-shell analysis of the EXAFS data, shows the presence of a non-statistical distribution of the different metal atoms in the nanoparticles. Specifically, we find that the Pt atoms in the particle show a pronounced tendency to self-segregate to surface sites.

The structural evolution seen during the condensation of the nanoparticles involved the initial nucleation of a close-packed structure followed by the inversion of the intra-particle distribution of the Pt and Ru atoms upon continued growth.[19] In this inversion, the core-segregated Pt atoms exchange with Ru surface atoms to form a surface Pt shell-structure. It is believed that the dynamic structural transformation revealed in this work is in large part a result of the strong influence that the finite size of the assembly imparts on the kinetics and overall energetics. In the nanoparticles prepared here, over 50% of the metals occupy surface (i.e., low coordination) sites. This bonding environment strongly directs a non-statistical partitioning of the metals species present in the nanoparticle. Of paramount interest is the demonstration made in this work of the facile reconstruction which occurs in nanoscopic metal crystals.

References

1. *Clusters and Colloids*; Schmid, G., Ed.; VCH, Weinheim, 1994.

2. Sinfelt, J. H. *Bimetallic Catalysts -- Discoveries, Concepts, and Applications*; Wiley: New York, 1983.

3. Tolles, W. M. In *Nanotechnology: Molecularly Designed Materials*; Chow, G.; Gonsalves, K. E., Eds.; ACS Symposium Series 622; American Chemical Society: Washington, DC, 1995; pp 1-18.

4. Mayer, J. W.; Lau, S. S. *Electronic Materials Science: For Integrated Circuits in Si and GaAs*; Macmillan: New York, 1990.

5. Andrews, M. P.; Ozin, G. A. *Chem. Mater.* **1989**, *1*, 174.

6. Freeman, D. L.; Doll, J. D. *Ann. Rev. Phys. Chem.* **1996**, *47*, 43.

7   Schwarz, J. A. In *Surface Segregation Phenomena*; Dowben, P. A.; Miller, A., Eds.; CRC Press: Boca Raton, Fl, 1990; Chapter 12.

8. Rodriquez, A.; Amiens, B.; Chaudret, P.; Casanove, M.-J.; Lacante, P.; Bradley, J. S. *Chem. Mater.* **1996**, *8*, 1978.

9. Cameron, D. S.; Hards, G. A.; Thomsett, D. In *Proc. Workshop on Direct Methanol-Air Fuel Cells*; Landgrebe, A. R.; Sen, R. K.; Wheeler, D. J., Eds.; Proceedings Series; The Electrochemical Society: Pennington, 1992; PV 92-14, pp 10-23.

10. Gasteiger, H. A.; Markovic, N. M.; Ross, P. N., Jr.; Cairns, E. J. *Electrochim. Acta* **1994**, *39*, 1825.

11. McBreen, J.; Mukerjee, S. *J. Electrochem. Soc.* **1995**, *142*, 3399.

12. Shapley, J. R.; Uchiyama, W. S.; Scott, R. A. *J. Phys. Chem.* **1990**, *94*, 1190.

13. Ichikawa, M. *Adv. Catal.* **1992**, *38*, 283.

14. Nashner, M. S.; Somerville, D. M.; Lane, P. D.; Adler, D. L.; Shapley, J. R.; Nuzzo, R. G. *J. Am. Chem. Soc.* **1996**, *118*, 12964.

15. Nashner, M. S.; Frenkel, A. I.; Adler, D. L.; Shapley, J. R.; Nuzzo, R. G. *J. Am. Chem. Soc.* **1997**, *119*, 7760.

16. Okamoto, H. In *Binary Alloy Phase Diagrams,* 2nd ed.; Massalski, T. B.; Okamoto, H.; Subramanian, P. R.; Kacprazate, L., Eds.; ASM: Materials Park, 1990; Vol. 3, p 2345.

17. *X-ray Absorption: Principles, Applications, Techniques of EXAFS, SEXAFS, and XANES*; Koningsberger, D. C.; Prins, R., Eds; Wiley: New York, 1988.

18. Zabinski, S. I.; Rehr, J. J.; Ankudinov, A.; Albers, R. C.; Eller, M. J. *Phys. Rev. B* **1995**, *52*, 2995.

19. Nashner, M. S.; Frenkel, A. I.; Shapley, J. R.; Nuzzo, R. G. to be submitted.